

Guanidine–Acylguanidine Bioisosteric Approach in the Design of Radioligands: Synthesis of a Tritium-Labeled N^G -Propionylargininamide ($[^3\text{H}]\text{-UR-MK114}$) as a Highly Potent and Selective Neuropeptide Y Y_1 Receptor Antagonist

Max Keller,[†] Nathalie Pop,[†] Christoph Hutzler,[†] Annette G. Beck-Sickinger,[‡] Günther Bernhardt,[†] and Armin Buschauer^{*,†}

Department of Pharmaceutical/Medicinal Chemistry II, Faculty of Chemistry and Pharmacy, University of Regensburg, Universitätsstrasse 31, D-93053 Regensburg, Germany, Institute of Biochemistry, University of Leipzig, Brüderstrasse 34, D-04103 Leipzig, Germany

Received August 13, 2008

Synthesis and characterization of (*R*)- N^{α} -(2,2-diphenylacetyl)- N -(4-hydroxybenzyl)- N^{ω} -([2,3- ^3H]-propanoyl)-argininamide ($[^3\text{H}]\text{-UR-MK114}$), an easily accessible tritium-labeled NPY Y_1 receptor (Y_1R) antagonist (K_B : 0.8 nM, calcium assay, HEL cells) derived from the (*R*)-argininamide BIBP 3226, is reported. The radioligand binds with high affinity (K_D , saturation: 1.2 nM, kinetic experiments: 1.1 nM, SK-N-MC cells) and selectivity for Y_1R over Y_2 , Y_4 , and Y_5 receptors. The title compound is a useful pharmacological tool for the determination of Y_1R ligand affinities, quantification of Y_1R binding sites, and autoradiography.

Introduction

Neuropeptide Y (NPY^a), a 36-amino acid peptide, is one of the most abundant neuropeptides in the central and peripheral nervous system. NPY is involved in the regulation of numerous (patho)physiological functions such as food intake, blood pressure, stress, pain, and hormone secretion. In humans, the biological effects of NPY are mediated by four receptor subtypes, termed Y_1 , Y_2 , Y_4 , and Y_5 . Recently, the Y_1 receptor (Y_1R) was reported to be expressed in different tumors such as breast cancer,¹ prostate cancer,² and adrenal tumors³ and therefore proposed as a potential tumor marker.⁴ The (*R*)-configured argininamide BIBP 3226 (**14**, Chart 1), the first highly potent and selective nonpeptide Y_1R antagonist,⁵ has been commonly used as a pharmacological tool for studying the physiological role of the Y_1R . The compound is considered a mimic of the C-terminus, i.e., Arg³⁵ and Tyr³⁶, in NPY.⁶ On one hand, the guanidino group in **14** has been considered important for the biological activity due to interaction with Asp²⁸⁷ of the human Y_1R ; on the other hand, the strongly basic group is a major drawback with respect to oral availability and brain penetration. Recently, we prepared a series of N^G -substituted derivatives of **14**, which revealed a preference for electron-withdrawing substituents in terms of retaining or even increasing the Y_1R affinity regardless of the by 4–5 orders of magnitude reduced basicity.⁷ Especially the introduction of carbamoyl residues into the N^G position yielded Y_1R antagonists with considerably increased affinity (Chart 1).^{7,8} These findings

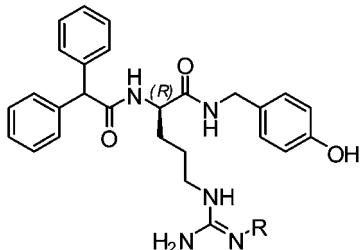
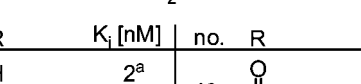
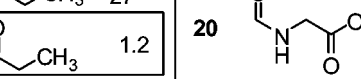
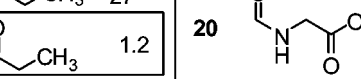
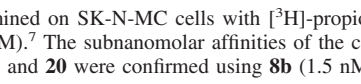
^a To whom correspondence should be addressed. Phone: +49-941 9434827. Fax: +49-941 9434820. E-mail: armin.buschauer@chemie.uni-regensburg.de.

[†] Department of Pharmaceutical/Medicinal Chemistry II, Faculty of Chemistry and Pharmacy, University of Regensburg.

[‡] Institute of Biochemistry, University of Leipzig.

^a Abbreviations: B_{\max} , maximum number of binding sites; CDI, carbonyldiimidazole; CRC, concentration–response curve; DCC, dicyclohexylcarbodiimide; EDAC, *N*-(3-dimethylaminopropyl)-*N'*-ethylcarbodiimide hydrochloride; DMAP, 4-(dimethylamino)pyridine; FAB, fast atom bombardment; FmocOSu, 9-fluorenylmethyl succinimidyl carbonate; H&E, hematoxylin and eosin; hPP, human pancreatic polypeptide; HR-MS, high resolution mass spectrometry; k_{ob} , observed association rate constant; k_{off} , dissociation rate constant; k_{on} , association rate constant; NPY, neuropeptide Y; PET, positron emission tomography; pNPY, porcine NPY; *rt*, room temperature; t_{R} , retention time; Y_1R , Y_2R , Y_4R , and Y_5R , NPY receptor subtypes Y_1 , Y_2 , Y_4 , and Y_5 .

Chart 1. Structures and Y_1R Affinities of BIBP 3226 (**14**) and Selected N^G -Substituted Derivatives, Arranged According to Increasing Size of the Substituent “R”

no.	R	K_I [nM]	no.	R	K_I [nM]
14	H	2 ^a	18		4.5 ^a
15		12 ^a	19		0.1 ^a
16		33 ^a	20		0.1 ^a
17		27 ^a	8a		1.2

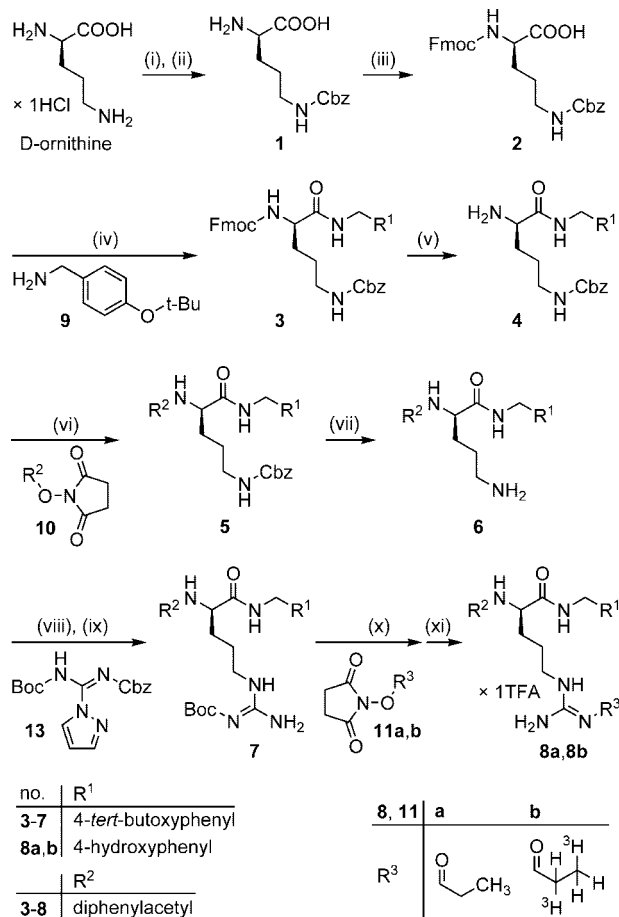
^a Determined on SK-N-MC cells with [^3H]-propionyl-pNPY as radioligand (1 nM).⁷ The subnanomolar affinities of the carbamoylated arginamides **19** and **20** were confirmed using **8b** (1.5 nM) as radioligand.

support the concept that the acylguanidines are bioisosteres of guanidines. The high affinities and selectivities achieved with this class of compounds prompted us to develop a Y_1R selective antagonistic radioligand.

Results and Discussion

N^G -Acetyl (**15**), N^G -methoxycarbonyl (**16**), and N^G -propyl (**17**) substituted argininamides (Chart 1) exhibit lower Y_1R affinities (two-digit nM range) than the parent compound BIBP 3226 (**14**), whereas the N^G -propionyl derivative **8a** turned out to be a highly potent Y_1 antagonist with an affinity of about 1 nM. Obviously, the extension of the acyl substituent by one methylene group enables an additional hydrophobic interaction, which compensates for the moderate acylation-induced decrease in affinity observed for the lower homologue **15**. This was also true for

Scheme 1. Synthetic Route for the Preparation of the N^G -Propanoyl Argininamides **8a,b**^a



^a Reagents and conditions: (i) Cbz-Cl (45% in toluene), NaOH 0.5 N, K_2CO_3 , $CuSO_4$, 20 h, 4 °C to rt; (ii) triplex III, H_2O , 60 min, 100 °C, 83%; (iii) FmocOSu, H_2O /dioxane, 20 h, rt, 96%; (iv) CDI, THF, 20 h, rt, 62%; (v) diethylamine, DCM, 4 h, rt, 76%; (vi) NEt₃, 1,2-dimethoxyethane, 20 h, 35 °C, 84%; (vii) Pd/C, ammonium formate, MeOH, 20 h, rt, 85%; (viii) NEt₃, CH_2Cl_2 , 20 h, rt; (ix) Pd/C, H_2 , MeOH, 3.5 h, rt, 84%; (x) NEt₃, MeCN, 20 h, rt; (xi) TFA, MeCN, 3 h, 50 °C, 70% (**8a**), 34% (**8b**).

the methoxycarbonyl derivative **16** ($K_i = 33$ nM) compared to the ethoxycarbonyl homologue **18** ($K_i = 4.5$ nM). Acylation was superior to alkylation at the N^G -position (**8a** vs **17**, Chart 1), but an exchange of the α -CH₂ group by an oxygen atom, resulting in an ester group, was again less favorable (**16**, **8a**, Chart 1). Surprisingly, the corresponding N^G -carbamoyl substituted analogues (**19**, **20**), containing a α -NH group, showed significantly higher affinities. Presumably, the presence of this H-donor group enables additional affinity-enhancing interactions, resulting in a different favorable orientation of the flexible amide substituent in **19**, **20** compared to the acyl residues in **8a,b**.

Considering Y₁R affinity and selectivity as well as synthetic feasibility, the N^G -[2,3-³H]-propionyl-substituted argininamide **8b** ([³H]-UR-MK114), the “hot” form of **8a**, was considered most attractive, particularly because tritiated propionic acid succinimidyl ester is commercially available as a radiolabeling reagent. In principle, this labeling strategy can be transferred to other classes of compounds containing guanidine as a pharmacophoric group.

Chemistry. Alkylguanidines are conventionally prepared from amines and bis-urethane (Boc, Cbz) protected guanidinylation reagents, for example, S-methyl isothioureas⁹ or pyrazol-1-carboxamidines^{10,11} or triflylguanidines.¹² Alternatively,

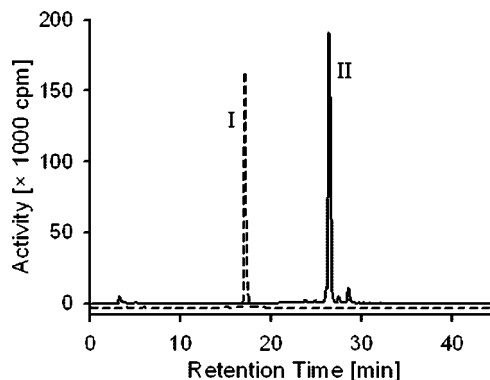


Figure 1. HPLC purity control of the freshly synthesized (I, dashed line) and long-term (18 months) stability control (II, solid line) of the tritiated Y₁R antagonist **8b** with radiometric detection, shown for different chromatographic conditions to avoid coincidence of the peaks. Conditions: I, purity control: eluent: mixtures of acetonitrile + 0.05% TFA (A) and 0.05% aq TFA (B), gradient: 0–30 min: A/B 20/80 to 90/10, 30–38 min: 90/10, $t_R = 16.7$ min; II, long term stability control: eluent: mixtures of acetonitrile (A) and 0.05% aq TFA (B), gradient: 0–30 min: A/B 20/80 to 50/50, 30–35 min: 50/50 to 90/10, 35–45 min: 90/10, $t_R = 26.5$ min. The identity of **8b** was confirmed by spiking with larger amounts of the “cold” analogue **8a**, which allowed UV detection.

Table 1. NPY Receptor Selectivity Data of **8a/b**

$Y_1 K_i$ [nM] ^a	$Y_2 K_i$ [nM] ^b	$Y_4 K_i$ [nM] ^c	$Y_5 K_i$ [nM] ^b
1.2	>10000	>10000	>2000

^a Binding of **8b** to SK-N-MC neuroblastoma cells. ^b Flow cytometric binding assay on CHO-Y₂ and HEC-1B-Y₅ cells using Dy-635-pNPY or Cy5-pNPY as labeled ligands (10 nM). ^c Flow cytometric binding assay on CHO-Y₄ cells and Cy5-[K⁴]-hPP as fluorescent ligand (5 nM).

guanidine derivatives can be *N*-alkylated with alcohols under Mitsunobu conditions.¹³ Acyl-substituted alkylguanidines are accessible if one of the protecting groups of the guanidinylation reagent is replaced with the pertinent acyl residue.⁸ However, such a synthetic route is not well suited for the preparation of a tritiated propionylguanidine because the radiolabel is preferably introduced in a final one-pot reaction. Therefore, direct attachment of the acyl substituent to the guanidine group in **14** (Chart 1) was performed using the N^G -Boc-*O*-*tert*-butyl protected analogue **7** as a precursor (Scheme 1). This method afforded the target compounds in good (up to 80%) yields and has been frequently used in our laboratory to synthesize N^G -acylated arginine derivatives. Carboxylic acids can be attached to the N^G -Boc-alkylguanidine scaffold with the aid of coupling reagents from peptide chemistry (EDAC, CDI) or using anhydrides, chlorides, and active esters. However, the reaction rate is noticeably slower compared to the coupling to amines.

The precursor **7** can be obtained from amine **6** by reaction with a guanidinylation reagent containing a Boc and a Cbz protecting group, followed by hydrogenolytic Cbz deprotection. For the preparation of amine **6**, starting from D-ornithine, the α -amino group was protected with Fmoc, orthogonally to Cbz and the *tert*-butyl phenyl ether.⁸ A conversion of the alcohol corresponding to amine **6** (obtained via reduction of D-glutamate) into acylated guanidines under Mitsunobu condition was reported not to give the desired argininamides¹⁴ and was therefore not explored any longer as an alternative synthetic route. The guanidinylation reagent **13** was prepared from aminoguanidine carbonate following reported protocols.¹⁰ All other required compounds (**9**, **10**, **11**) were prepared according to standard procedures.

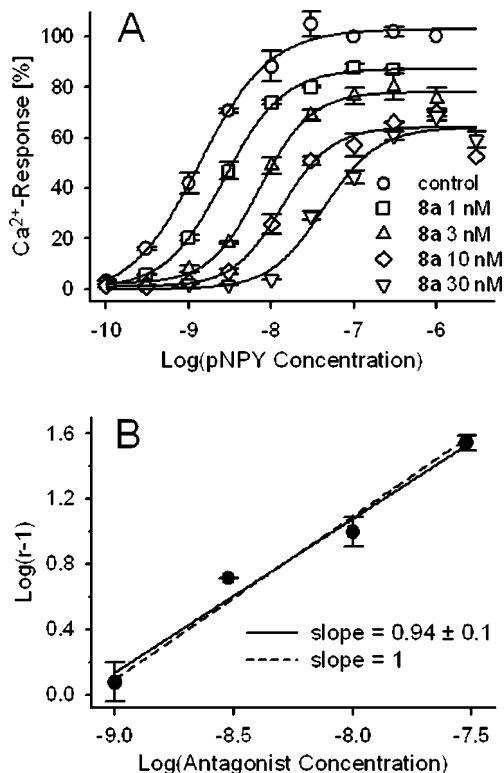


Figure 2. (A) Concentration–response curves (CRCs) of pNPY from a fura-2 assay on HEL cells. The presence of **8a** led to a parallel rightward shift of the curves. (B) Schild regression: $\log(r-1)$ plotted against $\log[\text{antagonist}]$; the concentration ratios r ($r = 10^{\Delta pEC50}$) were calculated from the rightward shifts ($\Delta pEC50$) of the CRCs in the presence of **8a** as shown in Figure 2A. The slope of the line equals unity, therefore the pA_2 value corresponds to pK_B : $pA_2 \approx pK_B = 9.1$ (slope forced to unity), $K_B = 0.8 \text{ nM}$ (mean values \pm SEM or propagated error, $n = 2$).

Depending on the source of succinimidyl [2,3-³H]-propionate, GE Healthcare (Amersham) and ARC (American Radiolabeled Chemicals, Inc.), the tritiated compound **8b** was obtained with specific activities of 97 Ci/mmol and 51 Ci/mmol, respectively. The radioligand **8b** was isolated by HPLC with a radiochemical purity of 99% (Figure 1, dashed line) and showed a high long-term stability when stored in ethanol at -20°C over a period of 1.5 years (Figure 1, solid line).

Pharmacology. The selectivity of the new Y_1 R antagonist **8a** for human NPY Y_1 over Y_2 , Y_4 , and Y_5 receptors was proven by flow cytometric binding assays based on fluorescence-labeled pNPY (Y_2 R, Y_5 R) or [K^4]-hPP (Y_4 R) according to previously described methods.^{15–17} As summarized in Table 1, comparable to the parent compound BIBP 3226, the N^G -propionylated derivative (**8a**) shows a clear binding preference for the Y_1 R.

The Y_1 R antagonism of **8a** was investigated in a fura-2-based Ca^{2+} -assay on HEL cells.¹⁸ Concentration–response curves of pNPY were constructed in the absence and presence of **8a** at different concentrations (Figure 2A), and the data were subjected to Schild analysis¹⁹ (Figure 2B). Because the slope in this linear plot nearly equals unity, a competitive antagonism of **8a** is very likely. The pK_B (in this case identical to pA_2) reflects the affinity of the antagonist and the resulting K_B value (0.8 nM) is in very good agreement with the K_D value (1.2 nM) from saturation binding experiments (Figure 3). A plausible reason for the depressed maxima of the concentration effect curves (Figure 2A) is hemi-equilibrium.¹⁹ Because of the rapid onset of the calcium response in the functional assay, the time window is too narrow to enable an equilibrium among the receptors, the

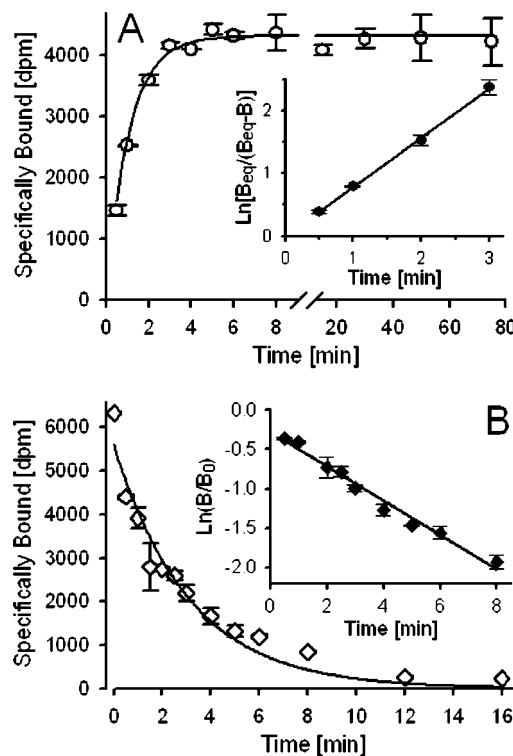


Figure 3. Association and dissociation kinetics for the specific Y_1 R binding of **8b** on SK-N-MC cells (65th passage) at 24°C . (A) Radioligand ($c = 3 \text{ nM}$) association as a function of time, Inset: $\ln[B_{\text{eq}}/(B_{\text{eq}} - B)]$ versus time, slope = $k_{\text{ob}} = 0.79 \text{ min}^{-1}$, $k_{\text{on}} = (k_{\text{ob}} - k_{\text{off}})/[L] = 0.19 \text{ min}^{-1} \cdot \text{nM}^{-1}$. (B) Radioligand (pre-incubation: 6 nM) dissociation as a function of time, monophasic exponential decay, $t_{1/2} = 2.2 \text{ min}$, Inset: $\ln(B/B_0)$ versus time, slope(-1) = $k_{\text{off}} = 0.22 \text{ min}^{-1}$. Mean values \pm SEM, $n = 3$.

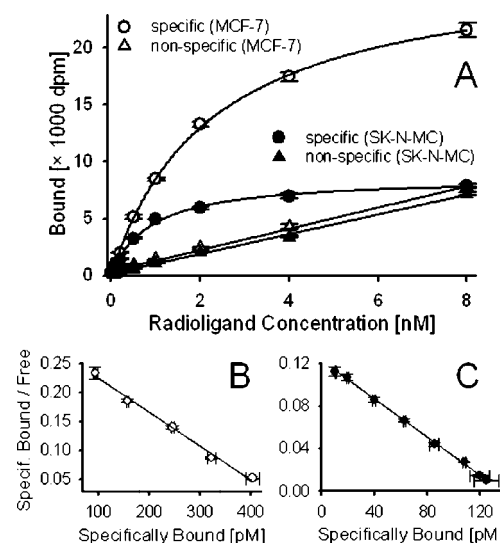


Figure 4. (A) Saturation curves for binding of **8b** to MCF-7 (176th passage) and SK-N-MC (67th passage) cells revealing K_D values of 2.2 nM and 0.85 nM, respectively. Estimated B_{max} (sites/cell): 120000 (MCF-7) and 52000 (SK-N-MC). The cell number was determined in at least 4–6 wells. (B) Scatchard plot for the binding of **8b** to MCF-7 cells, $K_D = -1/\text{slope} = 1.7 \text{ nM}$. (C) Scatchard plot for the binding to SK-N-MC cells, $K_D = -1/\text{slope} = 1.1 \text{ nM}$ (mean values \pm SEM or propagated error, $n = 3$).

agonist pNPY (slow binding kinetics²⁰) and the antagonist **8a** (high on- and off-rate, Figure 3).

The results of kinetic studies of **8b** at 24°C are presented in Figure 3. Association and dissociation at the Y_1 R were in the

Table 2. Y₁R Binding and Functional Characteristics of **8a/8b**

K_D [nM] ^a	K_D [nM] ^b	K_B [nM] ^c	K_D [nM] ^d	k_{on} [min ⁻¹ ·nM ⁻¹] ^e	k_{off} [min ⁻¹] ^f
2.9 ± 0.4	1.2 ± 0.1	0.8 ± 0.1	1.1 ± 0.1	0.19 ± 0.01	0.22 ± 0.01

^a Equilibrium dissociation constant determined on MCF-7 cells, mean value ± SEM from 5 independent experiments, each in triplicate. ^b Equilibrium dissociation constant determined on SK-N-MC cells, mean value ± SEM from 6 independent experiments, each in triplicate. ^c Schild analysis derived dissociation constant of **8a**, mean value ± SEM from 2 independent experiments (calcium assay using HEL cells). ^d Kinetically derived dissociation constant ± propagated error. ^e Association rate constant ± standard error from linear regression. ^f Dissociation rate constant ± standard error from linear regression.

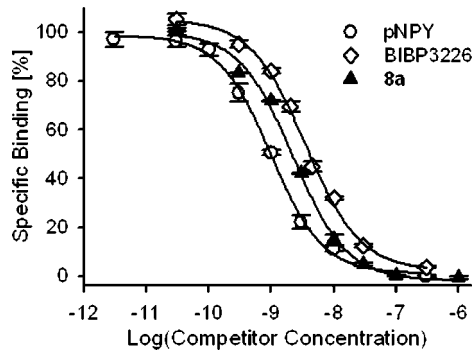


Figure 5. Displacement of the tritiated Y₁R antagonist **8b** ($c = 1.5$ nM) by the agonist pNPY, the antagonist BIBP 3226 and the nonlabeled analogue **8a**. The competition assay was performed on SK-N-MC cells at 24 °C with incubation periods of 20 min (BIBP 3226, **8a**) and 120 min (pNPY). BIBP 3226: $pIC_{50} = 8.44$, $K_i = 1.5$ nM; pNPY: $pIC_{50} = 9.01$, $K_i = 0.5$ nM. **8a**: $pIC_{50} = 8.65$, $K_i = 1.0$ nM (mean values ± SEM, $n = 3$).

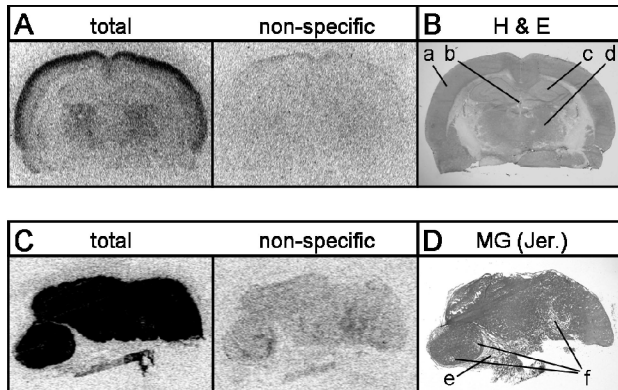


Figure 6. (A) Total and nonspecific binding of the tritiated Y₁R antagonist **8b** to adjacent coronal sections of rat brain (male Wistar rat, 10 month old). (B) H & E stained adjacent section, (a) cerebral cortex, (b) third ventricle, (c) hippocampus, (d) thalamus. (C) Total and nonspecific binding of **8b** to adjacent tumor sections (sc human MCF-7 mammary carcinoma from a NMRI (nu/nu) mouse). (D) Masson–Goldner (Jerusalem's modification) stained adjacent tumor section, (e) connective and adipose tissue, (f) necrotic regions.

range of minutes ($k_{on} = 0.19$ min⁻¹·nM⁻¹, $k_{off} = 0.22$ min⁻¹) as typical for antagonists. The kinetically derived K_D ($k_{off}/k_{on} = 1.1$ nM) is in excellent agreement with the K_D from saturation binding experiments (1.2 nM).

Saturation analysis of radioligands provides dual information, the equilibrium dissociation constant K_D and the maximum number of binding sites (B_{max}). Multiple saturation experiments with **8b** on SK-N-MC neuroblastoma cells and MCF-7 breast cancer cells afforded K_D values of 1.2 and 2.9 nM, respectively (Figure 4). The B_{max} value for SK-N-MC cells of about 50000 sites per cell fit well with data from literature.²¹ The breast

cancer cells express about 100000–150000 sites/cell (fluctuations are probably caused by a slightly varying estrogen stimulus provided by the fetal calf serum supplement of the culture medium). Estrogen stimulation of MCF-7 cells leads to Y₁R up-regulation to 300000 sites/cell. Y₁R up-regulation has been already reported on the mRNA level²² and could be confirmed on intact cells at the protein level using the radioligand **8b** as an NPY Y₁R probe. On the basis of these results, an assay has been developed for the functional characterization of estrogens and antiestrogens (to be reported elsewhere). Binding and functional Y₁R data of **8a/8b** are summarized in Table 2.

Competition binding experiments of **8b** with the antagonist BIBP 3226 and the agonist pNPY yielded K_i values (1.5 ± 0.2 nM and 0.5 ± 0.02 nM, respectively) consistent with reported data (Figure 5).^{21,23}

To explore the applicability of **8b** to autoradiographic binding studies cryosections of a human MCF-7 tumor, subcutaneously grown in a nude mouse, and of a rat brain were incubated with the new radioligand. In rat brain, Y₁R binding sites were clearly detected in the cerebral cortex in layers I–III (I: molecular layer; II: external granular layer; III: layer of medium-sized pyramidal cells), in the thalamus, and in the hippocampus (Figure 6A,B) as reported from binding studies with [¹²⁵I][Leu³¹,Pro³⁴]PYY and [³H]-BIBP3226.^{24,25} The results indicate a very high Y₁R expression in the tumor, as there is a strong difference between total and non-specific binding (Figure 6C).

Conclusion

N^G -propionylation of BIBP 3226 leads to a highly potent and selective Y₁R antagonist (**8a**). Direct N^G -acylation of N^G -Boc, *O*-tert-butyl protected BIBP 3226 (**7**) allows a convenient preparation of a tritium-labeled radioligand from succinimidyl [2,3-³H]-propionate with specific activities of up to 100 Ci/mmol. Because of the practicability and low costs of this labeling strategy, **8b** ([³H]-UR-MK114) is a highly attractive alternative to (the formerly commercially available) [³H]-BIBP 3226. **8b** has also advantages over radiolabeled peptides addressing the Y₁R due to stability, selectivity, mode of action (antagonist), and costs. [³H]-UR-MK114 can be used for the quantification of Y₁R binding sites as well as for autoradiography experiments on tissues. Because of the attenuated basicity ($pK_a = 7$ –8) of the acyl guanidine moiety, **8a** is supposed to exhibit an improved pharmacokinetic profile over the strongly basic BIBP 3226 ($pK_a \approx 13$). Generally, radioligands capable of penetrating into the brain would provide interesting tools for the study of Y₁R binding by ex vivo (autoradiography) and in vivo (PET) experiments. Recent findings in the NPY Y₂R¹⁴ as well as in the histamine H₂R and H₄R field²⁶ support the hypothesis that the concept of guanidine–acylguanidine bioisosterism may be of general interest to design receptor ligands including radiotracers with high affinity, reduced basicity and improved pharmacokinetic properties.

Experimental Section

(R)-N^α-(2,2-Diphenylacetyl)-N-(4-hydroxybenzyl)-N^ω-(2,3-³H-propanoyl)argininamide (8b). Here, only a brief experimental protocol is given. A more detailed procedure is provided as Supporting Information. **8b** was prepared from two different batches of succinimidyl-[2,3-³H]-propionate (**11b**), one from GE Healthcare (Amersham) provided in toluene (185 MBq/5 mL, $a_s = 3.48$ TBq/mmol), and a second one from American Radiolabeled Chemicals provided in ethyl acetate (185 MBq/1 mL, $a_s = 2.22$ TBq/mmol). The labeling reaction was performed in a 1.5 mL Eppendorf reaction vessel (screw top) in acetonitrile using 40 equiv of the labeling precursor **7**. NEt₃ was added to ensure deprotonation of **7**. A portion

of this mixture (precursor **7** and NEt_3) was added to the solution of **11b** in either toluene or ethyl acetate, and the solvents were removed by a slight stream of nitrogen and in a vacuum concentrator, respectively. The residue was dissolved in acetonitrile ($\approx 80 \mu\text{L}$) and remaining fractions of **7** and NEt_3 were added. The reaction mixture was stirred at rt for 20 h, then TFA was added and stirring was continued under moderate heating ($\approx 50^\circ\text{C}$) for 2–3 h. **8b** was purified by reversed-phase HPLC (column: Agilent Scalar C18, 250 mm \times 4.6 mm, 5 μm). The quantity was calculated from an HPLC standard curve (**8a**) and the specific activity was determined to be 3.6 and 1.9 TBq/mmol, respectively. **8b** is stored in ethanol with a TFA additive (100 μM) at -20°C . Yield of purified product: 34% and 33%, respectively (the actual efficiency of the labeling with the GE Healthcare product was about 60% related to the amount of activity, which was available after the toluene removal). Radiochemical purity (HPLC): 99% (Figure 1).

Data Analysis. All data to be fitted were processed with SigmaPlot 9.0. Data from saturation experiments were evaluated by one-site saturation fits (K_D , B_{\max}). Rate constants (k_{ob} , k_{off}) were analyzed using linear plots and simple linear regressions. The association rate constant (k_{on}) was calculated from k_{ob} , k_{off} and the radioligand concentration according to the correlation: $k_{\text{on}} = (k_{\text{ob}} - k_{\text{off}})/[\text{radioligand}]$. Data from competition experiments and agonist effect curves were analyzed by four-parameter sigmoidal fits. IC_{50} values were converted to K_i values using the Cheng–Prusoff equation.²⁷ For Schild analysis $\log_{10}(r - 1)$ was plotted against $\log_{10}[\text{antagonist}]$ with $r = 10^{\Delta EC_{50}}$. Raw data from flow cytometric experiments were processed with the aid of the WinMDI 2.7 software. All error bars in the diagrams represent the standard errors of the means or errors calculated by propagation of the uncertainties. The retention (capacity) factor was calculated according to $k = (t_R - t_0)/t_0$.

Acknowledgment. We are grateful to Dr. Thilo Spruss for the preparation of the cryosections, to Dr. Chiara Cabrele for the synthesis of pNPY, to Matthias Freund for synthetic help, to Elvira Schreiber, Susanne Bollwein, Brigitte Wenzl, and Franz Wiesenmeyer for expert technical assistance, and to Laura Emmerich and Dorothea Wedler for their assistance in the Schild analysis. This work was supported by the Graduate Training Program (Graduiertenkolleg) GRK 760, “Medicinal Chemistry: Molecular Recognition–Ligand–Receptor Interactions”, of the Deutsche Forschungsgemeinschaft.

Supporting Information Available: General experimental conditions, experimental details and analytical data for **8a**, intermediates and building blocks **1–7** and **9–13**, chromatogram of **8a** (purity control), detailed experimental procedure for the synthesis of **8b**, and pharmacological methods. This material is available free of charge via the Internet at <http://pubs.acs.org>.

References

- Reubi, J. C.; Gugger, M.; Waser, B.; Schaefer, J. C. Y(1)-mediated effect of neuropeptide Y in cancer: breast carcinomas as targets. *Cancer Res.* **2001**, *61*, 4636–4641.
- Magni, P.; Motta, M. Expression of neuropeptide Y receptors in human prostate cancer cells. *Ann. Oncol.* **2001**, *12* (2), S27–S29.
- Körner, M.; Waser, B.; Reubi, J. C. High expression of neuropeptide Y receptors in tumors of the human adrenal gland and extra-adrenal paranganglia. *Clin. Cancer Res.* **2004**, *10*, 8426–8433.
- Körner, M.; Reubi, J. C. NPY receptors in human cancer: a review of current knowledge. *Peptides* **2007**, *28*, 419–425.
- Rudolf, K.; Eberlein, W.; Engel, W.; Wieland, H. A.; Willim, K. D.; Entzeroth, M.; Wienen, W.; Beck-Sickinger, A. G.; Doods, H. N. The first highly potent and selective nonpeptide neuropeptide Y Y₁ receptor antagonist: BIBP3226. *Eur. J. Pharmacol.* **1994**, *271*, R11–R13.
- Sautel, M.; Rudolf, K.; Wittneben, H.; Herzog, H.; Martinez, R.; Munoz, M.; Eberlein, W.; Engel, W.; Walker, P.; Beck-Sickinger, A. G. Neuropeptide Y and the nonpeptide antagonist BIBP 3226 share an overlapping binding site at the human Y₁ receptor. *Mol. Pharmacol.* **1996**, *50*, 285–292.
- Hutzler, C. Synthese und pharmakologische Aktivität neuer Neuropeptid Y Rezeptorliganden: Von *N,N*-disubstituierten Alkanamiden zu hochpotenten Y1-Antagonisten der Argininamid-Reihe. Doctoral Thesis. University of Regensburg, Regensburg, Germany, 2001.
- Brennauer, A.; Dove, S.; Buschauer, A. Structure–Activity Relationships of Nonpeptide Neuropeptide Y Receptor Antagonists. *Handb. Exp. Pharm.* **2004**, *162*, 506–537.
- Gers, T.; Kunc, D.; Markowski, P.; Izdebski, J. Reagents for efficient conversion of amines to protected guanidines. *Synthesis* **2004**, *37*–42.
- Bernatowicz, M. S.; Wu, Y.; Matsueda, G. R. Urethane protected derivatives of 1-guanyl-pyrazole for the mild and efficient preparation of guanidines. *Tetrahedron Lett.* **1993**, *34*, 3389–3392.
- Drake, B.; Patek, M.; Lebl, M. A convenient preparation of mono-substituted *N,N*-di(BOC)-protected guanidines. *Synthesis* **1994**, *579*–582.
- Feichtinger, K.; Zapf, C.; Sings, H. L.; Goodman, M. Diprotected Triflylguanidines: A New Class of Guanidinylation Reagents. *J. Org. Chem.* **1998**, *63*, 3804–3805.
- Feichtinger, K.; Sings, H. L.; Baker, T. J.; Matthews, K.; Goodman, M. Triurethane-Protected Guanidines and Triflyldiurethane-Protected Guanidines: New Reagents for Guanidinylation Reactions. *J. Org. Chem.* **1998**, *63*, 8432–8439.
- Brennauer, A. Acylguanidines as bioisosteric groups in argininamide-type neuropeptide Y Y₁ and Y₂ receptor antagonists: synthesis, stability and pharmacological activity. Doctoral Thesis. University of Regensburg, Regensburg, Germany, 2006.
- Schneider, E.; Keller, M.; Brennauer, A.; Hoefelschweiger, B. K.; Gross, D.; Wolfbeis, O. S.; Bernhardt, G.; Buschauer, A. Synthesis and characterization of the first fluorescent nonpeptide NPY Y₁ receptor antagonist. *ChemBioChem* **2007**, *8*, 1981–1988.
- Schneider, E.; Mayer, M.; Ziernik, R.; Li, L.; Hutzler, C.; Bernhardt, G.; Buschauer, A. A simple and powerful flow cytometric method for the simultaneous determination of multiple parameters at G protein-coupled receptor subtypes. *ChemBioChem* **2006**, *7*, 1400–1409.
- Ziernik, R.; Brennauer, A.; Schneider, E.; Cabrele, C.; Beck-Sickinger, A. G.; Bernhardt, G.; Buschauer, A. Fluorescence- and luminescence-based methods for the determination of affinity and activity of neuropeptide Y₂ receptor ligands. *Eur. J. Pharmacol.* **2006**, *551*, 10–18.
- Müller, M.; Knieps, S.; Geselle, K.; Dove, S.; Bernhardt, G.; Buschauer, A. Synthesis and neuropeptide Y₁ receptor antagonistic activity of *N,N*-disubstituted ω -guanidino- and ω -aminoalkanoic acid amides. *Arch. Pharm. (Weinheim)* **1997**, *330*, 333–342.
- Kenakin, T. P. *A Pharmacology Primer: Theory, Applications, and Methods*, 2nd ed.; Academic Press: New York, 2007.
- Vanderheyden, P. M.; Van Liefde, I.; de Backer, J. P.; Vauquelin, G. [³H]-BIBP3226 and [³H]-NPY binding to intact SK-N-MC cells and CHO cells expressing the human Y₁ receptor. *J. Recept. Signal Transduct. Res.* **1998**, *18*, 363–385.
- Entzeroth, M.; Brauner, H.; Eberlein, W.; Engel, W.; Rudolf, K.; Wienen, W.; Wieland, H. A.; Willim, K. D.; Doods, H. N. Labeling of neuropeptide Y receptors in SK-N-MC cells using the novel, nonpeptide Y₁ receptor-selective antagonist [³H]BIBP3226. *Eur. J. Pharmacol.* **1995**, *278*, 239–242.
- Amlal, H.; Faroqui, S.; Balasubramaniam, A.; Sheriff, S. Estrogen up-regulates neuropeptide Y Y₁ receptor expression in a human breast cancer cell line. *Cancer Res.* **2006**, *66*, 3706–3714.
- Michel, M. C.; Beck-Sickinger, A.; Cox, H.; Doods, H. N.; Herzog, H.; Larhammar, D.; Quirion, R.; Schwartz, T.; Westfall, T. XVI. International Union of Pharmacology recommendations for the nomenclature of neuropeptide Y, peptide YY, and pancreatic polypeptide receptors. *Pharmacol. Rev.* **1998**, *50*, 143–150.
- Gehlert, D. R.; Gackenheimer, S. L. Differential distribution of neuropeptide Y Y₁ and Y₂ receptors in rat and guinea-pig brains. *Neuroscience* **1997**, *76*, 215–224.
- Dumont, Y.; St-Pierre, J. A.; Quirion, R. Comparative autoradiographic distribution of neuropeptide Y Y₁ receptors visualized with the Y₁ receptor agonist [¹²⁵I][Leu³¹,Pro³⁴]PYY and the nonpeptide antagonist [³H]BIBP3226. *Neuroreport* **1996**, *7*, 901–904.
- Ghorai, P.; Kraus, A.; Keller, M.; Götte, C.; Igel, P.; Schneider, E.; Schnell, D.; Bernhardt, G.; Dove, S.; Zabel, M.; Elz, S.; Seifert, R.; Buschauer, A. Acylguanidines as bioisosteres of guanidines: N^G -acylated imidazolylpropylguanidines, a new class of histamine H₂ receptor agonists. *J. Med. Chem.* **10.1021/jm800841w**.
- Cheng, Y.; Prusoff, W. H. Relationship between the inhibition constant (K_I) and the concentration of inhibitor which causes 50 per cent inhibition (I₅₀) of an enzymatic reaction. *Biochem. Pharmacol.* **1973**, *22*, 3099–3108.